American Journal of Advanced Research, 2024, 8–2
December. 2024, pages 01-09
doi: 10.5281/zenodo.13862545
http://www.ibii-us.org/Journals/AJAR/
ISBN 2572-8849 (Online), 2572-8830 (Print)

Simulation and Modeling of Steam Methane Reformation Utilizing Nickel-Based Catalyst

Brett Rice and Jun Xu*

Department of Mechanical, Environmental, and Civil Engineering, Mayfield College of Engineering, Tarleton State University, TX 76401

*Email: junxu@tarleton.edu

/Received on 06/05/2024; revised on 09/27/2024; published on 9/30/2024

Abstract

Our methodology started with an extensive review of the literature on Steam Methane Reformation (SMR) systems, establishing a foundation for anticipated outcomes while pinpointing gaps in essential fluid or geometric conditions. These gaps were then filled using standardized values from existing literature. We employed two methodologies for system modeling and optimization. Initially, Ansys Chemkin was utilized to solve SMR mathematical models utilizing the plug-flow reactor model, thereby determining optimal operational parameters such as temperature, pressure, and catalyst geometric dimensions (diameter and length). Subsequently, these optimized parameters were integrated into models of both single-catalyst pipes and multi-catalyst pipes, which underwent simulation using the Computational Fluid Dynamics (CFD) software ANSYS Fluent. Preliminary findings suggest that optimal operating conditions for SMR fall within the range of 800 – 1000°C and 25-28 bar, with expected fluid velocities reaching up to 20 m/s under these conditions. Corresponding dimensions for the catalyst tube within these parameter ranges were determined to be 49 mm in length and 176 mm in inner diameter. By validating the efficacy of SMR and identifying potential enhancements, the rationale for installing more SMR reactors in both new and existing facilities is justified. This strategic expansion facilitates the more efficient utilization of resources, thereby contributing to our capacity to meet the continuously escalating energy demands of the present and future.

Keywords: Steam Methane Reformation, Water Gas Shift, ANSYS, Fluent, Chemkin, Reactor, Computation Fluid Dynamics, Hydrogen, Methane, Steam, Nickel, Catalyst

1 Introduction

Energy in the form of electricity, heat, or work will always be in demand. As of 2022, a significant 79 percent of electricity generation in the United States relied on non-renewable energy sources, comprising oil (28%), natural gas (33%), coal (10%), and nuclear energy (8%) (U.S. Energy Information Administration). Today, these non-renewable energy sources are abundant, coming in from every corner of the world and sustaining the United States' energy needs. However, non-renewable energy has two critical flaws. First is the environmental impact that non-renewable sources such as gas and oil have on the environment. The second is the finite supply of non-renewable sources. The method of non-renewable energy source production, by nature, requires an unreasonable length of time to regenerate. It takes far too long to be sustainable. To prepare for and replace non-renewable energy shortages, more renewable methods of energy production have been developed. Better-known methods of renewable energy sources include hydroelectric, solar heating and electricity production, wind turbines, and hydrogen generation. One of these methods, hydrogen generation, has been shown to have immense potential to produce high-quality clean energy in a brief time. Hydrogen production can be achieved through several methods. The first method is through fuel cells, which consume water and electricity to create oxygen and hydrogen. Fuel cells are great for collecting hydrogen and oxygen in small-scale plants. On large-scale plants, fuel cells can have efficiency and performance issues. Another method utilizes gases called hydrocarbons along with water vapor and reforms the gases through the application of heat and pressure to generate hydrogen. This method is called Steam Methane Reformation (SMR), and this paper serves to model SMR production of

hydrogen through mathematical modeling and simulations using ANSYS Chemkin and Fluent. Hydrogen reformation is a chemical process in which a hydrocarbon, which can be methane (CH_4), is put through a reactor containing a catalyst that chemically breaks down the hydrocarbon and steam and reforms it into hydrogen, carbon dioxide, and carbon monoxide molecules. The separated hydrogen atoms will be collected through a filtering process and stored for future use. With ANSYS Chemkin, the chemical consumption and production of each molecule species within the feed gas can be modeled with respect to the gas' position within the reactor. On the other hand, ANSYS Fluent is used to map the energy transfer and fluid properties of the gas as it travels through the reactor. Using both, a valid model of the reformer can be created to see the viability and shortcomings of SMR to better understand and develop it for future energy needs.

1.1 Literature Review

Steam methane reformation is not a new practice. Since as early as 1913, research has been going into how to better extract hydrogen molecules from common hydrocarbons. Some methods to produce syngas, such as coke gasification, had already existed before SMR. Three companies, BASF, ICI, and Standard Oil, have been credited as the first to research and develop SMR technology (Murkin and Brightling, 2016). In 1928, BASF started research into SMR hydrogen production started in the town of Billingham UK. There BASF had created a patent for a steam reformer utilizing a nickel-based catalyst. Research would continue until 1936 when the patent would result in the first commission steam methane reformer plant. In response to this development, two companies that had also been researching steam reformers, FG Farben and Standard Oil, had entered an agreement to collaborate on stream reformation research to catch up with BASF's progress. This collaboration resulted in three steam methane reformers located in Bayway, USA, and later an additional three steam reformers in Baton Rouge, USA (Lee). The first steam reformers utilized externally heated tubes to heat the stock gas and catalyst to force a chemical reaction. The first steam reformer had an operating pressure and temperature of 1-4 bar and 730-800^{o}C (Murkin and Brightling, 2016). Like any initial system, the first steam reformers were not yet optimized. The original steam reformer had required operation parameters of 1-4 bar and 730-800^{o}C, while modern SMR reactors can operate comfortably between the operating parameters 900-1200 K for temperature and 3.5 – 28 bar for pressure. This initial limitation in strength was due to the construction and hardware of the first SMR reactor. As new materials were developed utilizing better strength and heat resistance, new SMR reactors allowed for more extreme operating conditions. Current reformer tubes now utilize centrifugally cast high alloy steels with high creep rupture strength (Steam Reformer Tubes). These materials allowed for the reactor tubes to manage higher operating conditions while also decreasing the tube's thickness. Another improvement in the SMR process is through the catalyst. The first catalysts used in reforming were typically nickel bases. The choice to use this catalyst turned out to be the right one since, even today, nickel-based catalysts are still used. While still capable of reacting with the feed gas, the reaction rate and efficiency of the reforming process with the cubic catalyst were much less than ideal. This was due to most of the catalysts material not being in contact with the feedstock gas. Later ICI soon developed a tubular catalyst shape that would be known as the Raschig ring shape, a common shape of catalyst used today (Lee). The feed gas would flow through and over the cylindrical shape of the catalyst and the reaction rate of the gas would increase. Several more catalyst shapes were developed, each improving the surface area to volume ratio of the catalyst. These include 4-hole cylindrical pellets, the Quadra lobe cylindrical pellets, and the Citadel SSR cylindrical foil-supported structure.

Before reforming the biogas-natural gas mixture, it must first be filtered to remove any impurities (Ashraf et al., 2018). Impurities with the gas mixture can include dirt particles and non-hydrocarbon gases that got through previous filtering procedures. A more substantial issue occurs when the gas mixture includes gases composed of sulfur. When sulfur gets into the reformer reactor, a chemical reaction can occur that allows the material ZnO to chemically bond with the sulfur. ZnO is a component that is found in the anodes and cathode of the reformer. The sulfur catalytically converts from thiols, thiophenes, or COS, into H_2S which is absorbed by the catalyst (Mokhatab et al., 2015). It is vital that the maximum amount of dihydrogen sulfide gas contained within the gas mixture does not exceed than four parts per million (PPM) (Mokhatab et al., 2015). In the case that the sulfur PPM is greater than the maximum limit, the sulfur gas will react with the nickel-based catalyst and other types of catalyst and degrade it. This is referred to as poisoning the catalyst (Mokhatab et al., 2015, Enayatizade et al., 2019). When a catalyst is poisoned, it is left in an inert state where chemical reactions are partially or completely stopped. This makes sulfur filters even more important as they not only increase the effectiveness of SMR hydrogen production but also prevent expensive catalyst failure and costly repairs.

For larger-scale reformers, it is common to see several pre-reformer reactors along with the main reformer reactor. This is to ensure that hydrogen is extracted from the feed gas before being disposed of properly. *Figure 1* shows both the pre and post-reformer. Both follow the same principles as the primary reformer but with two additional benefits. The first benefit of the pre-reformer also serves to prepare the feed gas by heating it to a more appropriate temperature, around 800 to 1000 degrees Celsius, or to increase the working fluid's pressure somewhere within 25-28 bar (Nobandegani et al., 2021). The second benefit that comes with both reformers is that the general hydrogen production efficiency is increased with each additional reformer reactor. Overall, fitting an SMR reactor with a pre-reformer can increase the hydrogen production efficiency by 8-10%, while fitting the reactor with a post-reformer will increase the efficiency by up to approximately 30% (Debottlenecking hydrogen, 2023).

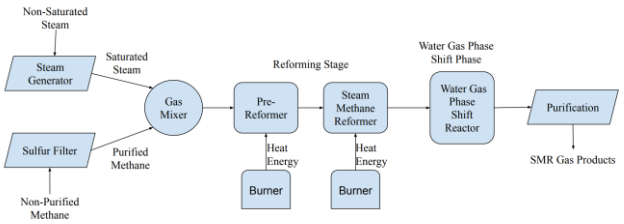

Figure 1: Reforming system with pre-reformer and secondary(post)-reformer

2 Materials and Methods

2.1 Mathematical Model

This paper will focus on modeling and simulating a single catalyst to better understand the mechanics behind Steam Methane Reformation (SMR). SMR is a process that breaks down the chemical bonds of methane and water vapor and reassembles the components to create usable hydrogen and waste carbon monoxide and carbon dioxide molecules. Many varieties of reformers exist. Each of these can utilize different catalysts, stock gas, and parameters to produce hydrogen. For this study, a nickel-based catalyst will be used in mathematical modeling and simulation due to its extensive experimental evaluation. Even with a determined catalyst material, the quantity of hydrogen production can change depending on the design and operating parameters. These parameters can be geometry dependent as shown in Figure 2, catalyst diameter, length, surface area, etc., or operation parameters, pressure, and temperature. Typically, the range of the parameters in terms of temperature and pressure range from 800 - 1000 degrees Celsius and from 5 - 35 bar or MPa (Nobandegani et al., 2021). With these ranges being so high, it would be unsafe to construct an SMR reactor incorrectly, and it would be expensive to have one bought and inspected. Instead, the focus will be shifted to creating a mathematical and visual model of the SMR through programs such as ANSYS Chemkin and ANSYS Fluent. The process in which each program is used is explained using the flow chart shown in *Figure 3*. An ideal model of an SMR reactor can be created using existing experimental data to obtain an estimation of a simple SMR reactor to generate process reaction rate, hydrogen yield per volume, and hydrogen conversion efficiency. The general shape of the reactor used in modeling is shown in *Figure 2* (Peymanfard et al., 2023). The reactor's geometric parameters are listed in *Table 1*. The model shows a simple cylindrical tube that makes up the catalyst and the outside shell. Steam, methane, and heat energy are injected into the inner cylindrical space where it reacts with the catalyst. In this setup, some of the methane and steam will move through the system without reacting. In a typical SMR system, additional reactors are added to catch and reform any non-reacted gas. The gas that does react is to be converted into hydrogen, carbon dioxide, or carbon monoxide. Hydrogen that is produced is either removed from the main gas stream through filters or the gas can transport itself through the porous catalyst into another stream of pure hydrogen. According to Xu and Froment, several catalyst types can be used for SMR; however, their effectiveness is varied (Xu and Froment, 1989). One of the most common catalyst types, the one used in the Xu and Froment model, is a nickel-based material. The breakdown and reforming reactions that occur within the Xu and Froment nickel-based catalyst are listed in *Table 2* where the coefficients A, β, and E correspond to *Equation 1*. (Richter et al., 2023) Because the process relies on the surface area of the catalyst, it is common for multiple reactors to be linked to ensure that the maximum amount of hydrogen is generated. Using reaction rate relations for an ideal chemical equation for SMR, a model can be made. By understanding SMR reactions, it is possible that this method of energy production can be further refined to become suitable for practical applications. By producing more hydrogen, it becomes possible to make use of the benefits of an increased supply of hydrogen, such as increasing the utilization of fuel cell technology and cleaner burning hydrogen combustion processes.

$$k_{fi} = A_i T^{\beta_i} \exp\left(\frac{-E_i}{R_c T}\right) \quad (1)$$

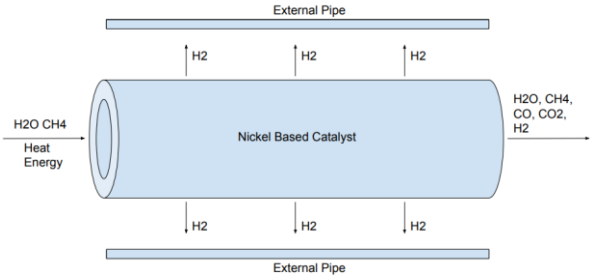

Figure 2: Basic SRM reactor diagram

Table 1: Plug Flow reactor Parameters.

Reactor Parameters	
Inside Diameter	10 mm
Outside Diameter	14 mm
Length	30 mm
Temperature	800-1000°C
Pressure	25-28 bar
Mass Flow Rate	2 kg/s

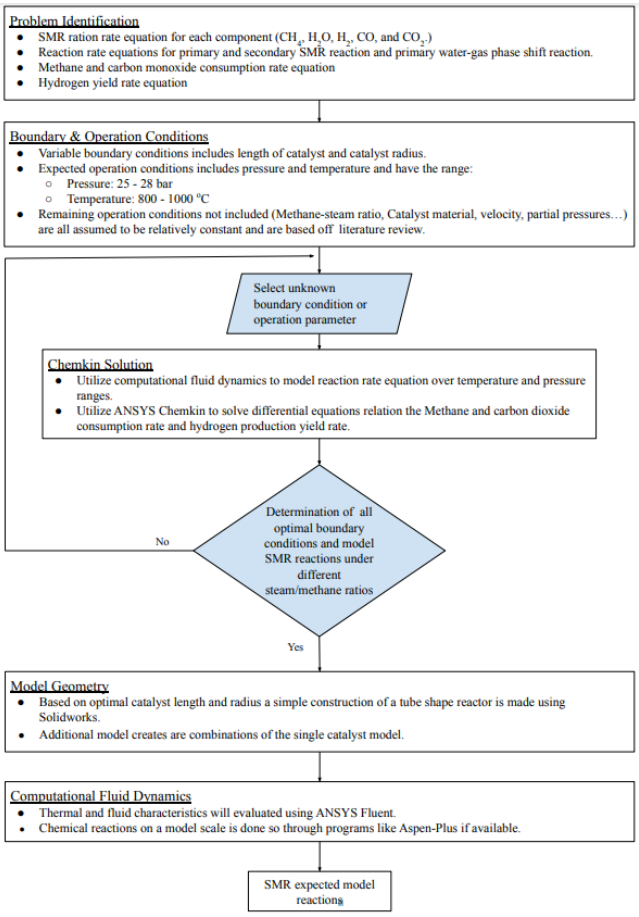

Figure 3: SMR process flowchart

Table 2: Surface Kinetics Reactions and Coefficients

Reaction	A (mol*cm*s*K)	β	E (kJ/mol)
$H_2O + Ni(S) \Rightarrow O(S) + H_2 + Ni(B)$	$1.00 \cdot 10^{-1}$	0.000	0.0
$CH_4 + Ni(S) \Rightarrow CH_4(S) + Ni(B)$	$8.00 \cdot 10^{-3}$	0.000	0.0
$CH_4(S) + Ni(S) \Rightarrow CH_3(S) + H(S) + Ni(B)$	$1.54 \cdot 10^{+22}$	0.087	55.8
$CH_3(S) + Ni(S) \Rightarrow CH_2(S) + H(S) + Ni(B)$	$1.54 \cdot 10^{+24}$	0.087	98.1
$CH_2(S) + O(S) + Ni(B) \Rightarrow CH_2O(S) + Ni(B)$	$3.70 \cdot 10^{+24}$	0.087	95.2
$CH_2O(S) + Ni(S) \Rightarrow CHO(S) = H(S) + Ni(B)$	$3.09 \cdot 10^{+23}$	−0.087	57.2
$CHO(S) + Ni(S) \Rightarrow CO(S) = H(S) + Ni(B)$	$3.71 \cdot 10^{+21}$	0.000	0.0
$CO(S) + Ni(B) \Rightarrow CO + Ni(S)$	$3.56 \cdot 10^{+11}$	0.000	111.2
$CO_2(S) + Ni(B) \Rightarrow CO_2 + Ni(S)$	$6.44 \cdot 10^{+7}$	0.000	25.9
$2H(S) + Ni(B) \Rightarrow H_2(S) + Ni(S)$	$2.54 \cdot 10^{+20}$	0.000	95.2
$H_2(S) + Ni(B) \Rightarrow H_2 + Ni(S)$	$3.00 \cdot 10^{-2}$	0.000	5.0

At the foundation of SMR, the reformation and water-gas phase reaction can be reduced and described with three chemical equations. *Table 3* lists the three primary equations that the steam and methane undergo to become carbon monoxide, carbon dioxide, and hydrogen. Both reformation equations are endothermic meaning that they require heat energy for the reaction to function. Reaction two is for the additional water gas phase shift reaction that not only produces more hydrogen from excess and added water vapor, but it also removes harmful carbon monoxide and replaces it with the less harmful gas carbon dioxide.

Table 3: Stochiometric Equations of SMR and WGS

Reaction #	Reaction Type	Stochiometric equation	Activation Energy, ΔH, (kJ/kmol)
1	SMR	$CH_4 + H_2O \Leftrightarrow CO + 3H_2$	$-2.061 * 10^5$
2	WGS	$CO + H_2O \Leftrightarrow CO_2 + H_2$	$4.11 * 10^4$
3	SMR	$CH_4 + 2H_2O \Leftrightarrow CO_2 + 4H_2$	$-1.65 * 10^5$

These chemical reactions show the ideal inputs and outputs of the SMR system. What the equations do not show is how the system works. SMR reactors are complicated systems that depend on half a dozen variables. These variables can include the materials used for the catalyst, the operational parameters of the SMR reactor, to the type of feed gas used, all of which can affect the yield and purity of hydrogen production. A challenge and limitation of SMR research is that understanding the kinematic equation of a particular catalyst can rely heavily on experimental analysis and

data with models having more favorable extensive testing than others. Favoring one model over others may lead to a false understanding of one model's importance over another. To prevent this, multiple models were taken into consideration for relations and simulations. Requirements for the model to be considered are needed to define the reaction rates for the hydrogen and methane for each chemical equation. along with a model for the hydrogen yield and the efficiency of the SMR process. Both mathematical modal and graphical models were considered to understand SMR best.

A model proposed by Wang, Zhu, and Lin provided a model that has ample mathematical modeling; however, the proposed physical model did not fit the need of the simulation as well as other options (Wang et al., 2016). On the other hand, the models proposed by Harald Malerød-Fjeld et al. had excellent experimental setup and result delivery; however, without mathematical modeling, the simulation of the model would be more difficult (Malerød-Fjeld et al., 2017). A model proposed by Xu and Froment not only has both extensive experimental results and mathematical modeling, but it has also become a general guide to dozens of published SMR research papers because of its extensive testing and multifunctional application to various feed gas and operating parameters (Xu and Froment, 1989). This model provides the yield of hydrogen, and the reaction rates for the SMR and water-gas shift reaction process have been determined. The reaction rates describe the number of moles that are produced with respect to the catalyst mass and time. The reaction rates equations in *Table 4* describe the number of moles of the reactant that are transformed into the product through the stoichiometric equation shown in *Table 3*. (Wang et al., 2016).

Table 4: Reaction Rate Equations for SMR and WGR Reactions

Reaction	Reaction Rate (kmol / kg_cat h)
$r_1 \begin{pmatrix} Steam\ Methane \\ Reaction\ 1 \end{pmatrix}$	$\frac{k_1}{p_{H_2}^{2.5} * DEN^2} * \left(p_{CH_4} * p_{H_2O} - \frac{p_{H_2}^3 * p_{CO}}{K_{eq_1}} \right)$
$r_2 \begin{pmatrix} Water\ Gas\ Phase \\ Reaction\ 2 \end{pmatrix}$	$\frac{k_2}{p_{H_2}^{2.5} * DEN^2} * \left(p_{CO} * p_{H_2O} - \frac{p_{H_2} * p_{CO_2}}{K_{eq_2}} \right)$
$r_3 \begin{pmatrix} Steam\ Methane \\ Reaction\ 3 \end{pmatrix}$	$\frac{k_3}{p_{H_2}^{3.5} * DEN^2} * \left(p_{CH_4} * p_{H_2O}^2 - \frac{p_{H_2}^4 * p_{CO_2}}{K_{eq_3}} \right)$

Table 5: Reaction Rate Equations for Reactants/Products

Reactant/Product	Reaction Rate (kmol / kg_cat h)
CH_4	$r_1 + r_3$
H_2O	$r_1 + r_2 + 2r_3$
CO	$r_1 - r_2$
CO_2	$-(r_2 + r_3)$
H_2	$-(3r_1 + r_2 + 4r_3)$

The reaction rates each depend on the partial pressure of gas species reacting in the SMR process as well as an experimental constant K_{eq_i} and k_i. The parameter DEN and the partial pressure are shown with *Equation 2* and *Equation 3* (Wang et al., 2016).

$$DEN = 1 + K_{CH_4} * p_{CH_4} + K_{CO} * p_{CO} + K_{H_2} * p_{H_2}^{0.5} + K_{H_2O} * \frac{p_{H_2O}}{p_{H_2}} \quad (2)$$

$$P_i = y_i P \quad i = CH_4, H_2, H_2O, CO, CO_2 \quad (3)$$

The reaction rates are experimentally derived relationships developed using the Xu and Froment model. (Xu and Froment, 1989). Three sets of coefficients explain the absorption kinetic rates and their relationship to temperature. *Table 6, Table 7, and Table 8* all show the component absorption, chemical equation, and the equilibrium coefficient for each of the reaction rate equation in *Table 4* and *Table 5* (Li et a., 2019).

These coefficients create a connection between the temperature of the fluid and the reaction rate of the catalyst. By increasing the temperature, the values of the coefficients could increase or decrease resulting in a change in the rate of reaction. Both the chemical reactions *Table 4*, as well as each species component in the stochiometric reaction equations are represented. The coefficients K_{eq_1}, K_{eq_2}, and K_{eq_3} are different in that they determine when the designated reaction reaches a state of equilibrium. By increasing the temperature of the fluid, the equilibrium coefficient values, or the state in which the reaction rates reach equilibrium are changed. The reaction rates given in *Table 4* represent the three chemical stochiometric processes for SMR and WGS. Furthermore, these reaction rates can be further subdivided into reaction rates representing the individual components. *Table 5* shows the rection rate between the components CH_4, H_2O, H_2, CO, and CO_2 (Wang et al., 2016).

These reaction rates are the sum of the species component from the SMR and WGS equations. Positive values refer to the component being a product, or produces value, while negative values refer to the component being a consumed value. These equations are suitable to use for a catalyst that is

nickel based. The reaction rate for hydrogen is particularly useful to determine the quantity of hydrogen produced on a per catalyst mass and time scale.

Table 6: Absorption Coefficients

Symbols	Component Absorption Coefficients
k_{CH_4}	$6.65 * 10^{-9} \exp\left(-\frac{4604.28}{T}\right)$
k_{H_2O}	$1.77 * 10^{5} \exp\left(-\frac{10666.35}{T}\right)$
k_{CO}	$8.23 * 10^{-10} \exp\left(-\frac{8497.71}{T}\right)$
k_{H_2}	$6.12 * 10^{-14} \exp\left(-\frac{9971.13}{T}\right)$

Table 7: Chemical Equation Coefficients

Symbols	Chemical Equations Coefficients
k_1	$2.64 * 10^{14.5} \exp\left(-\frac{28879}{T}\right)$
k_2	$1.22 * 10^{-2} \exp\left(-\frac{8074.3}{T}\right)$
k_3	$6.63 * 10^{13.5} \exp\left(-\frac{29336}{T}\right)$

Table 8: Equilibrium Coefficients

Symbols	Equilibrium Coefficients
$K_{eq\,1}$	$10266.76 * 10^{6} exp\left(-\frac{26830}{T} + 30.114\right)$
$K_{eq\,2}$	$\exp\left(\frac{4400}{T} + 4.036\right)$
$K_{eq\,3}$	$K_{eq\,1} * K_{eq\,2}$

2.2 Catalyst Models

Three models have been created to represent the catalyst and the surrounding hydrogen space. The first model consists of a single catalysis and is shown with cover pipe, *Figure 4a*, and without, *Figure 4b*. The single catalyst model shows the most simplified case for the steam methane reformer. The external pipe shown in *Figure 4b* serves as a boundary for the hydrogen and has an inner diameter of 93 mm.

A)

B)

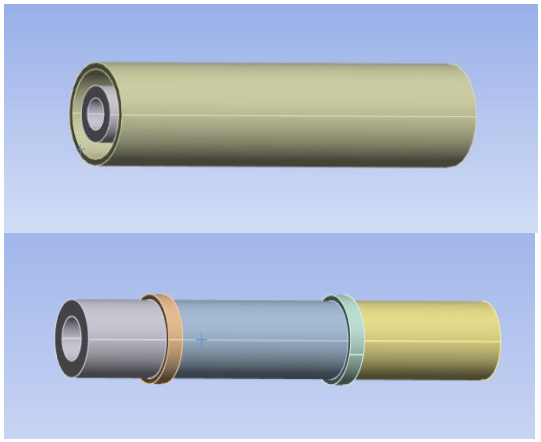

Figure 4: Catalyst (a) with and (b) without external pipe

Figure 2 shows the location of the inlet parameters as well as the outlet conditions applying to the single catalyst model. For the single-pipe and two-pipe models the inlet conditions applied to the surface of each catalyst surface equally, three times for the single pipe and six times for the two-pipe system. There should be only one pressure outlet for each model which is applied in the same location and with the same pressure conditions.

3 Results

ANSYS Chemkin is a program dedicated to modeling chemical reactions. For ANSYS Chemkin to properly operate four tasks must be completed. The first is the creation of the model used during the chemical process. In this model the inlet, outlet, and reactor type are all specified. In this model there is only one catalyst meaning that there is only one reactor. The parameters of this reactor are taken from *Table 1*. In this model a single gas inlet, a plug flow reactor, and a single gas outlet are defined. The second, third, and fourth task are you define the gas phase kinetics, surface phase kinetics, and thermodynamic property files. The gas phase kinetics file establishes the elements and molecule species used during the chemical process. It serves no other purpose since all reactions occur on the surface of the catalyst. The surface phase kinetics file is used to define all reactions occurring between the gas and the catalyst. The full breakdown and reforming process of the steam and methane needs to be described in this file. *Table 2* gives all possible stoichiometric equations that occur in an ideal steam methane reformation reactor. Lastly the thermodynamic property table self-defines all necessary thermodynamic information for each of the elements and molecule species used in the reaction and is provided in the Chemkin database. When the gas phase, surface phase, and thermodynamics files are created and imported and the reactor properties from

Table 1 are used, the reaction can then be simulated. *Figure 5*, *Figure 6*, and *Figure 7* all show the result of the chemical reaction occurring in the SMR process.

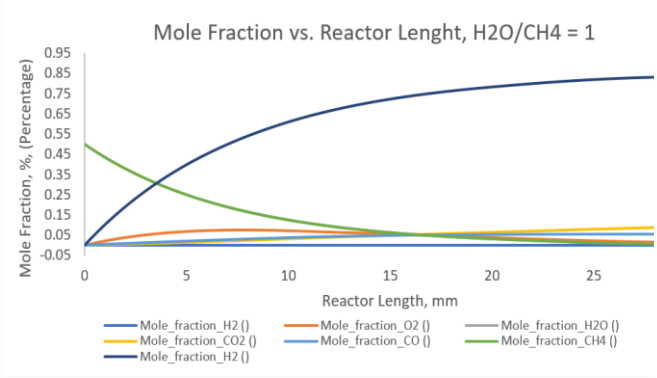

Figure 5: Mole Fraction vs Reactor Length for steam-carbon ratio 1

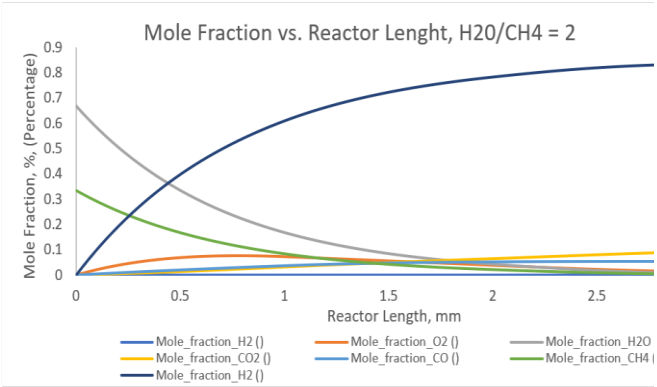

Figure 6: Mole Fraction vs Reactor Length for steam-carbon ratio 2

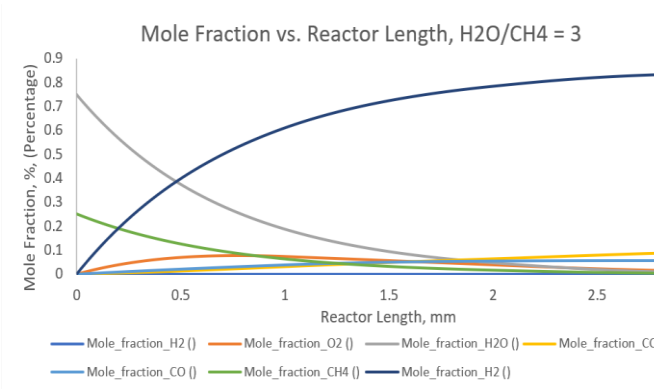

Figure 7: Mole Fraction vs Reactor Length for steam-carbon ratio 3

Figure 5, *Figure 6*, and *Figure 7* all show the mole fraction change of the feed gas as it travels through the reactor at the various H2O/CH4 ratios. In this simulation only steam and methane are present in the feed gas when the reactor length is zero. As the gas travels the team and methane are consumed and are converted. The results were compared to similarly created models (Możdzierz, et al., 2014, and Poliana et al., 2020) The comparison showed that all three models react the same way and validate each other.

3.1 Catalyst Simulation Results

Using Ansys Fluent, simulation results regarding the CFD and thermal properties of each of the three cases can be determined. *Figure 8*, *Figure 9*, and *Figure 10* show the contour charts of the hydrogen's velocity, pressure, and kinetic energy for a single catalyst.

Each of the systems were simulated under different mesh densities. A mesh structure that is integrated into the fluid space and is composed of elements. An element is a differential space in which all CFD and heat transfer equations are applied. Each element is calculated, with the end results is the combination of those element solutions. By affecting the size of the element, the density of the mesh is also affected. Smaller density mesh can be computed more quickly; however, they are not as accurate when compared to higher density mesh solutions. Due to the limitations of the Ansys student license, only a mesh with a density less than 518000 elements can be used. *Table 9* and *Table 10* show the results of each simulation under element sizes of 0.05 m, 0.01 m, 0.0075 m, and 0.005 m. An element size of 0.0075 m is necessary for *Table 9* and *Figure 10* due to its size. Pressure and temperature are consistent regardless of mesh density for *Figure 8*, *Figure 9*, and *Figure 10*. Velocity on the other hand slightly increases with each mesh.

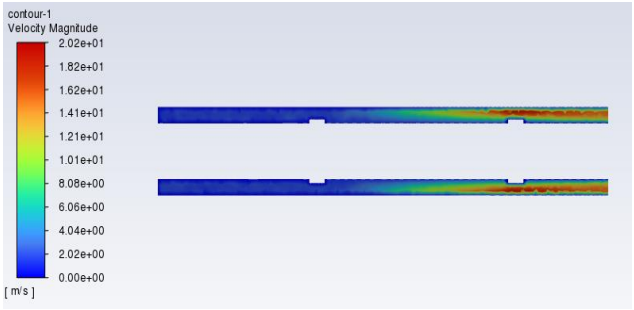

Figure 8: Single catalyst velocity.

The simulation is set up to only allow pure hydrogen in from the catalyst. By doing this, the catalyst diagram in *Figure 8* represents the first catalyst that the gas mixture is exposed to. As expected, the velocity of the fluid before reaching the catalyst is near zero. However, as focus moves towards the right of *Figure 8*, the velocity begins to build until it reaches a near maximum as the end of the catalyst. The velocity maximum is around 20.2 m/s or around 45 miles per hour.

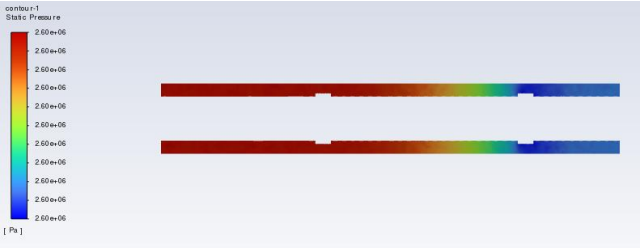

Figure 9: Single catalyst pressure.

The reason for the fluid's fast movements is due to the difference in pressure. The pressure exuded in the SMR reactor is set to be around 26 bar or 2.6 MPa. This is shown in *Figure 9*. With the addition of hydrogen from the catalyst, a small pressure difference is created. For *Figure 8*, this difference is small, only being around 2 kPa, however it is enough to influence the fluid into a steady flow.

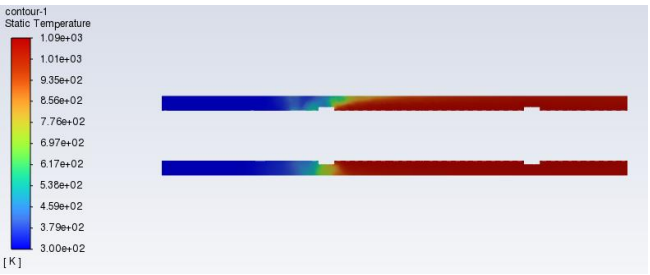

Figure 10: Single catalyst temperature.

The last parameter, temperature, is a byproduct of the SMR system. Heat energy is required for the SMR process to occur and so the temperature of the hydrogen is high. In *Figure 10*, it is seen that almost immediately the temperature of the fluid space increases to its maximum when the hydrogen gas permeates across the catalyst. The total results of the FEA analysis at each mech density are shown in *Table 9*.

Table 9: Single catalyst mesh and results.

Mesh Size	Max. Pressure [Pa]*10^6	Max. Velocity [m/s] * 10^1	Max. Temperature [K] * 10^3	Min. Temperature [K] * 10^2
0.05	2.60002050	1.8535	1.1529	2.9926
0.01	2.60002025	1.8937	1.1272	3.0000
0.005	2.60002200	2.0896	2.6002	2.5999

Following the result for the single catalyst model is the results for the single pipe model. This model is used to more accurately represent the change in fluid properties that are shown in a full scale SMR reactor due to them utilizing more than one catalyst. Overall, the behavior of each model does not change drastically. *Figure 11*, *Figure 12*, and *Figure 13* show the results for the single pipe system. The velocity, pressure, and temperature react similarly to the single catalyst results perfectly although the pressure difference is around 17 kPa instead of the original 2 kPa. The velocity of the hydrogen has now reached a maximum value of 61 m/s. This shows that the amount of hydrogen is building as the hydrogen continues from the start of the first catalyst to the end of the last. *Table 10* shows the total results and fluid properties of the three catalysts under each mesh density.

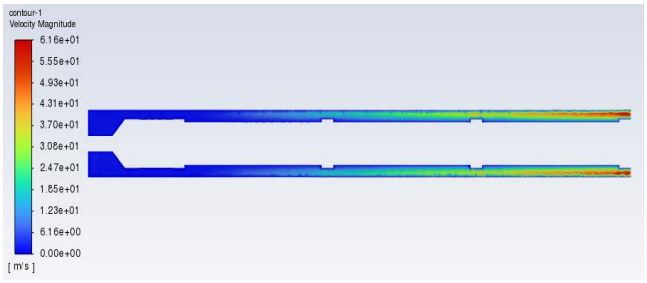

Figure 11: Single pipe velocity.

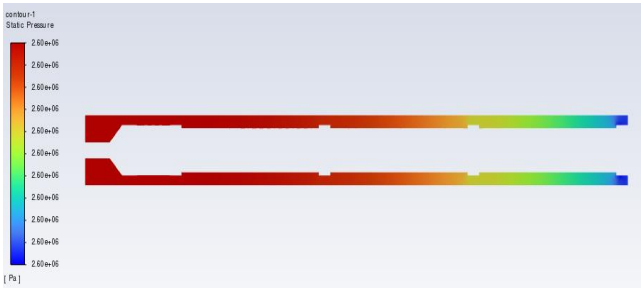

Figure 12: Single pipe pressure.

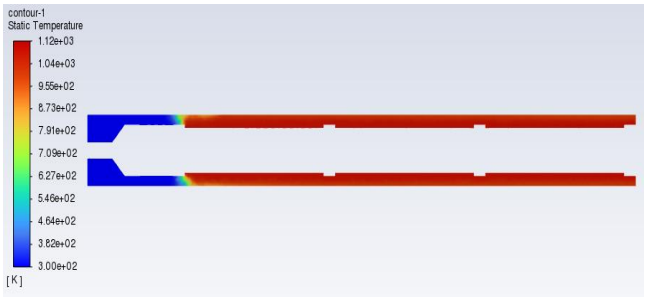

Figure 13: Single pipe temperature.

Table 10: Single pipe mesh and results.

Mesh Size	Max. Pressure [Pa]*10^6	Max. Velocity [m/s] * 10^1	Max. Temperature [K] * 10^3	Min. Temperature [K] * 10^2
0.05	2.60016850	4.8107	1.0750	1.0749
0.01	2.60017525	4.8758	1.0750	1.0749

0.00 5	2.60019 950	5.4398	1.0750	1.0749

4 Conclusion and Future Works

A major concern for environmentalists is the consequences of continuous fossil fuel usage including the environmental impact from extracting the fuel and the emissions caused by the fuel's usage. This rise in concern has in turn led to interest in alternative renewable sources of energy. Steam methane reformation is one renewable process that converts methane and steam into clean usable hydrogen gas fuel. The conversion process is done using a nickel-based catalyst stationed inside a pressurized furnace operating at a temperature range of 800 – 1000°C and a pressure range of 25-28 bar. The pretreated gas enters the SMR reactor contacting the catalyst. Under extreme pressure and heat the methane and steam begin a decomposition process, breaking the species into their base elements before reassembling the components into hydrogen, carbon dioxide, and carbon monoxide. Multiple reformers, Steam Methane or Water Gas Shift Reactors, can be utilized to maximize efficiency. One the reforming process is completed the remaining gas is filtered and separated where the usable hydrogen is stored, and the waste gas can be reutilized or discarded. By using programs such as ANSYS Chemin and Fluent, the expected model reaction for a standard nickel-based catalyst SMR reactor can be modeled. Chemkin utilizes the gas phase kinetics and surface phase kinetic properties of the catalyst and gas to model the decomposition process of methane and steam and reconstruct them into useful hydrogen gas, carbon monoxide, and carbon dioxide. Using this analysis, I can gain a general understanding of how effective a theoretical catalyst can be made. Following the chemical analysis, ANSYS Fluent was used to determine the computational fluid dynamics of expected syngas products. SMR is a complicated process, and there are many more tasks that could be done to better understand how SMR works. Future work considerations include the consideration of a physical experimental setup along with further analysis of the SMR process under difference parameter conditions including, change in catalyst material and geometric dimensions and application of different feed gas. In conclusion, while the transition from non-renewable energy sources may be difficult, understanding and utilizing SMR can provide numerous benefits—both environmental and economic—in the long run. By harnessing the power of SMR technologies, the energy produced in the future can be a cleaner, more resilient energy.

Acknowledgements

We express our gratitude to Dr. Hoe-Gil Lee for their assistance in ensuring the quality of this paper.

References

U.S. Energy Information Administration - EIA - independent statistics and analysis. U.S. energy facts explained - consumption and production - U.S. Energy Information Administration (EIA). (n.d.). https://www.eia.gov/energyexplained/us-energy-facts

Murkin, C., & Brightling, J. (2016). Eighty Years of steam reforming. *Johnson Matthey Technology Review*, *60*(4), 263–269. https://doi.org/10.1595/205651316x692923

Lee, S. (n.d.). *History of steam methane reforming (SMR)*. Scribd. https://www.scribd.com/document/234534909/Cre

Steam reformer tubes. Home - thyssenkruppp Uhde. (n.d.). https://www.thyssenkrupp-uhde.com/en/products-and-technologies/fertilizer-technologies/ammonia-plants/ammonia-technology-proprietary-equipment/steam-reformer-tubes

M. A. Ashraf, O. Sanz, M. Montes, and S. Specchia, "Insights into the effect of catalyst loading on methane steam reforming and controlling regime for metallic catalytic monoliths," *International Journal of Hydrogen Energy*, vol. 43, no. 26, pp. 11778–11792, Jun. 2018. doi: 10.1016/j.ijhydene.2018.04.126

S. Mokhatab, W. A. Poe, S. Mokhatab, W. A. Poe, and J. Y. Mak, "Chapter 3 - Basic Concepts of Natural Gas Processing," in *Handbook of Natural Gas Transmission and processing*, Third Edition., Waltham MA: Gulf Professional Publishing, 20115, pp. 123–135

H. Enayatizade, M. Chahartaghi, S. M. Hashemian, A. Arjomand, and M. H. Ahmadi, "Techno-economic evaluation of a new CCHP system with a hydrogen production unit," *International Journal of Low-Carbon Technologies*, vol. 14, no. 2, pp. 170–186, 2019. doi:10.1093/ijlct/ctz017

Debottlenecking hydrogen plant production capacity, https://www.digitalrefining.com/article/1000471/debottlenecking-hydrogen-plant-production-capacity (accessed Jun. 7, 2023).

Velazquez Abad, A., & Dodds, P. E. (2017). Production of hydrogen. Encyclopedia of Sustainable Technologies, 293–304. https://doi.org/10.1016/b978-0-12-409548-9.10117-4

M. Sinaei Nobandegani *et al.*, "One-dimensional modelling and optimization of an industrial steam methane reformer," *Chemical and Biochemical Engineering Quarterly*, no. 4, 2022. doi:10.15255/cabeq.2021.1963

Mohammad Javad Peymanfard, Alireza Sedaghat, "Mathematical Modeling Methods and Their Application in the System Analysis for Methanol Steam Reforming Process" *Chemical Process Design*, Vol.2 No.1. DOI: 10.22111/CPD.2023.44973.1017

Richter, J., Rachow, F., Israel, J., Roth, N., Charlafti, E., Günther, V., Flege, J. I., & Mauss, F. (2023). Reaction mechanism development for methane steam reforming on a ni/al2o3 catalyst. *Catalysts*, *13*(5), 884. https://doi.org/10.3390/catal13050884

Wang, B., Zhu, J., & Lin, Z. (2016). A theoretical framework for multiphysics modeling of methane fueled solid oxide fuel cell and analysis of low steam methane reforming kinetics. *Applied Energy*, *176*, 1–11. https://doi.org/10.1016/j.apenergy.2016.05.049

H. Malerød-Fjeld *et al.*, "Thermo-electrochemical production of compressed hydrogen from methane with near-zero energy loss," *Nature Energy*, vol. 2, no. 12, pp. 923–931, 2017. doi:10.1038/s41560-017-0029-4

Y. Li, Y. Chen, and J. Wu, "Enhancement of methane production in Anaerobic Digestion Process: A Review," *Applied Energy*, vol. 240, pp. 120–137, Apr. 2019. doi: 10.1016/j.apenergy.2019.01.243

Poliana P. S. Quirino, André Amaral, Karen V. Pontes, Francesco Rossi, and Flavio Manenti *Industrial & Engineering Chemistry Research* **2020** *59* (24), 11250-11264 DOI: 10.1021/acs.iecr.0c00456

Możdzierz, Marcin & Brus, Grzegorz & Sciazko, Anna & Komatsu, Yosuke & Kimijima, S. & Szmyd, Janusz. (2014). An attempt to minimize the temperature gradient along a plug-flow methane/steam reforming reactor by adopting locally controlled heating zones. Journal of Physics: Conference Series. 530. 012040. 10.1088/1742-6596/530/1/012040.

J. Xu and G. F. Froment, "Methane steam reforming, methanation and water-gas shift: I. Intrinsic Kinetics," *AIChE Journal*, vol. 35, no. 1, pp. 88–96, 1989. doi:10.1002/aic.690350109